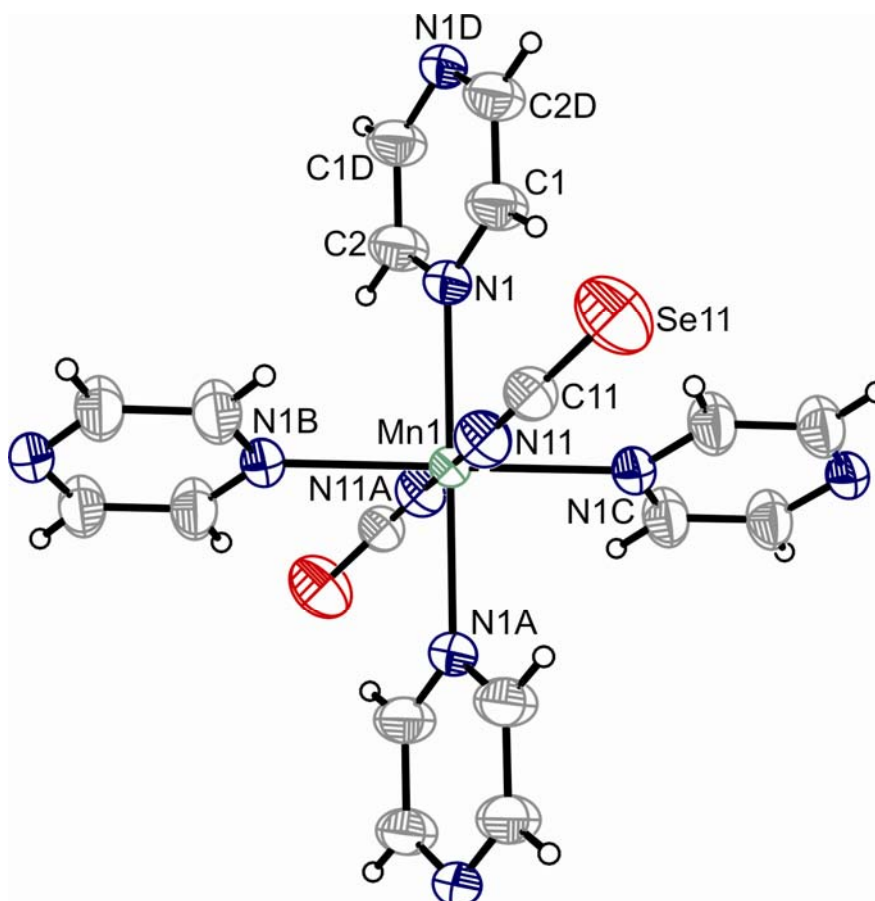


## Supporting Information

### Rational design of bridging selenocyanates by thermal decomposition reactions

**Mario Wriedt and Christian Näther\***

- Thermal ellipsoid plot for **1**.  
(Figure S1)
- DSC curve for **2**.  
(Figure S2)
- Rietveld difference plot for **2**.  
(Figure S3)
- IR spectroscopic data for **1** and **2**.  
(Figure S4 and S5)
- Experimental XRPD patterns for products obtained by reaction of different ratios of  $\text{Mn}(\text{NCSe})_2$  and pyrazine (4:1, 2:1, 1:1).  
(Figure S6)
- Experimental and calculated XRPD pattern for **1**.  
(Figure S7)
- Further experimental details.



**Figure S1.** Thermal ellipsoid plot of the crystal structure of  $[\text{Mn}(\text{NCSe})_2(\text{pyzz})_2]_n$  (**1**) with view of the coordination sphere of the metal cation with labeling and displacement ellipsoids drawn at the 50% probability level. Symmetry codes: A =  $-x, -y, -z + 1$ ; B =  $-x, y, -z + 1$ ; C =  $x, -y, z$ ; D =  $-x + 1/2, -y + 1/2, -z + 1$ .

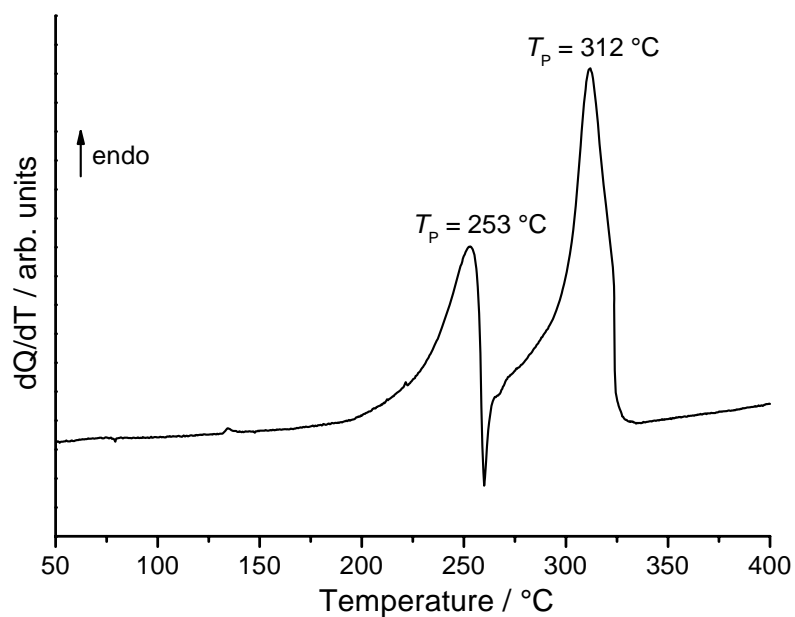


**Figure S2.** DSC curve of  $[\text{Mn}(\text{NCSe})_2(\text{pyz})_2]_n$  (1). Heating rate = 3 °C/min; given are the peak temperatures  $T_p$  (°C).

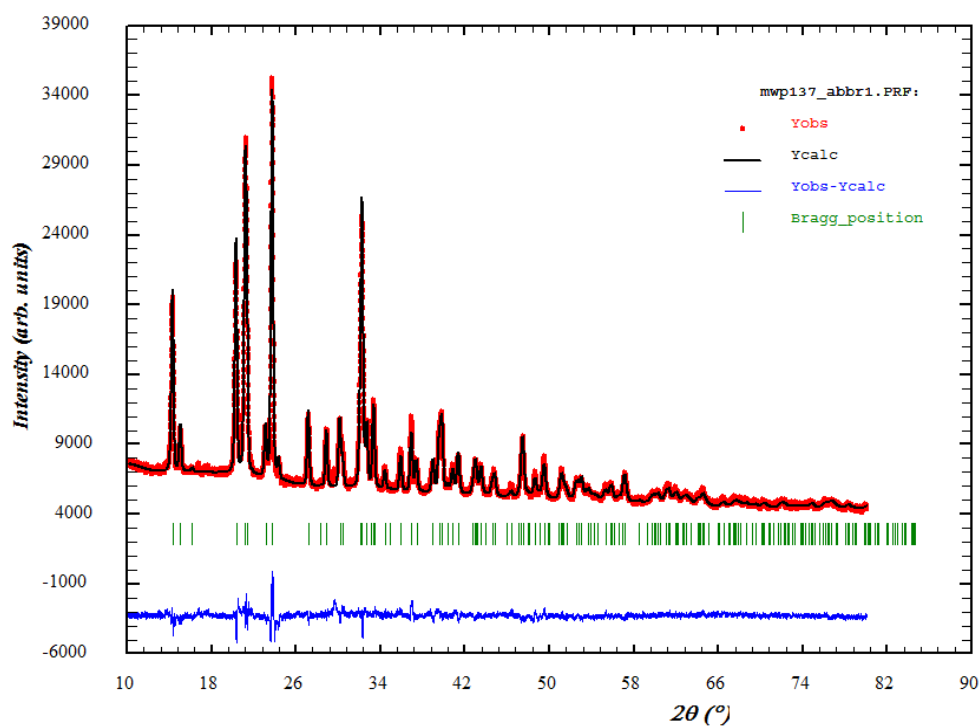


**Figure S3.** Difference plot of the Rietveld refinement of  $[\text{Mn}(\text{NCSe})_2(\text{pyz})_2]_n$  (2).

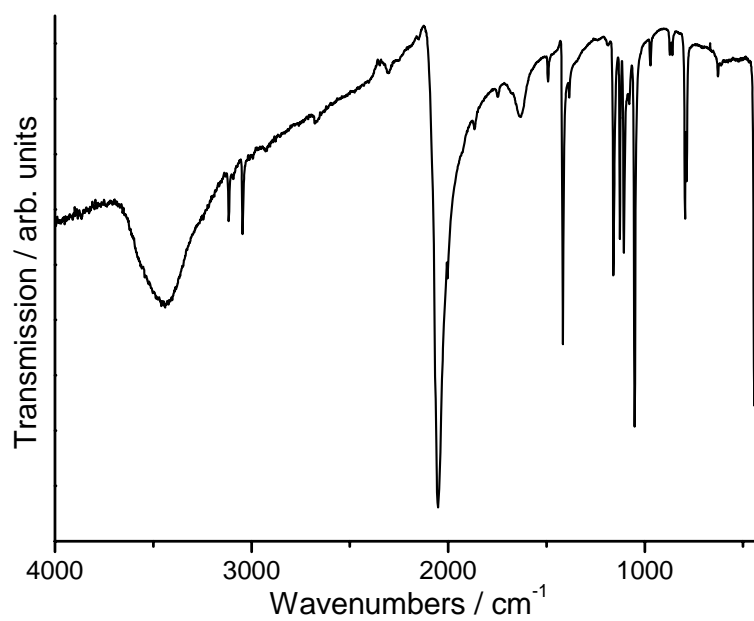


**Figure S4.** IR spectroscopic data of  $[\text{Mn}(\text{NCSe})_2(\text{pyZ})_2]_n$  (**1**).

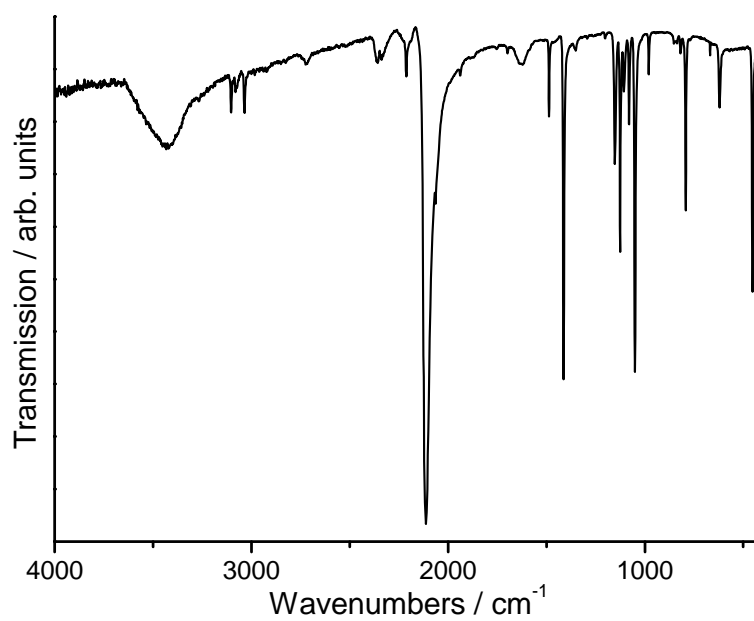


**Figure S5.** IR spectroscopic data of  $[\text{Mn}(\text{NCSe})_2(\text{pyZ})]_n$  (**2**).

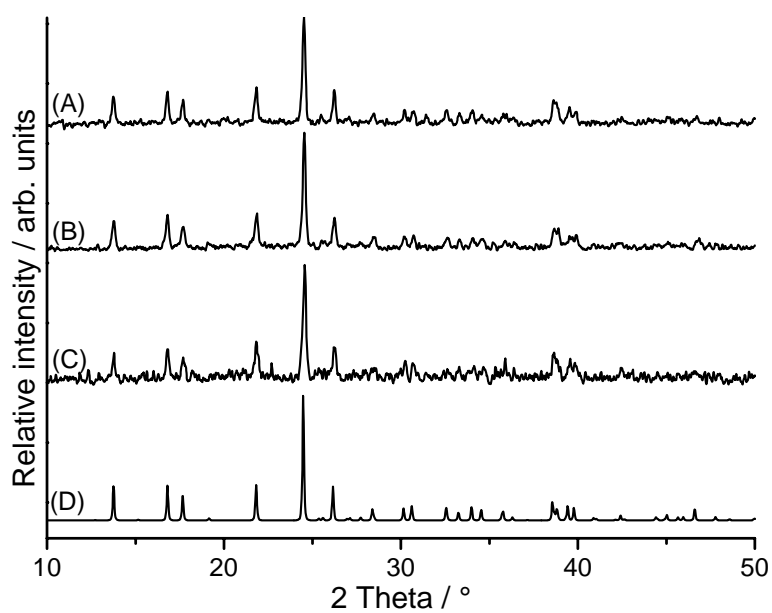


**Figure S6.** Experimental XRPD patterns for products obtained by reaction of different ratios of Mn(NCSe)<sub>2</sub> and pyrazine (A = 1:1, B = 2:1, C = 4:1) and XRPD pattern calculated from single crystal data (D) of [Mn(NCSe)<sub>2</sub>(pyz)<sub>2</sub>]<sub>n</sub> (**1**).

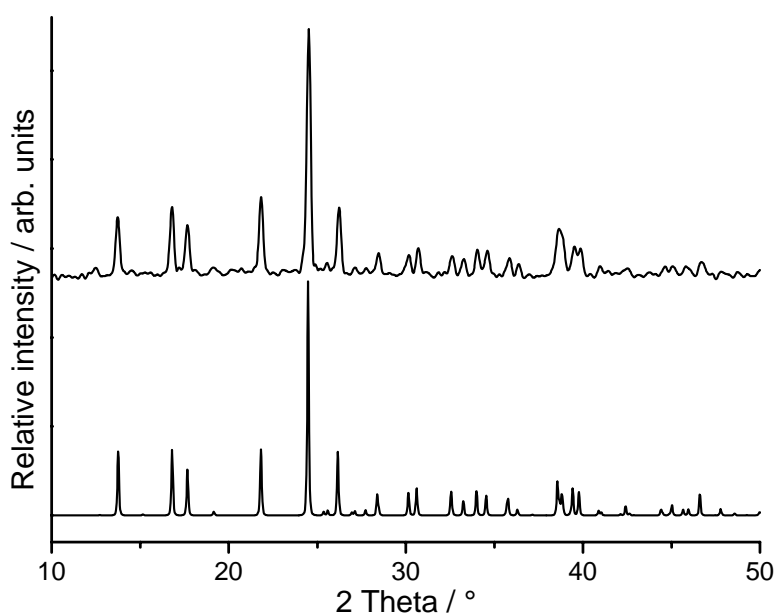


**Figure S7.** Experimental XRPD pattern (top) and XRPD pattern calculated from single crystal data (bottom) of [Mn(NCSe)<sub>2</sub>(pyz)<sub>2</sub>]<sub>n</sub> (**1**).

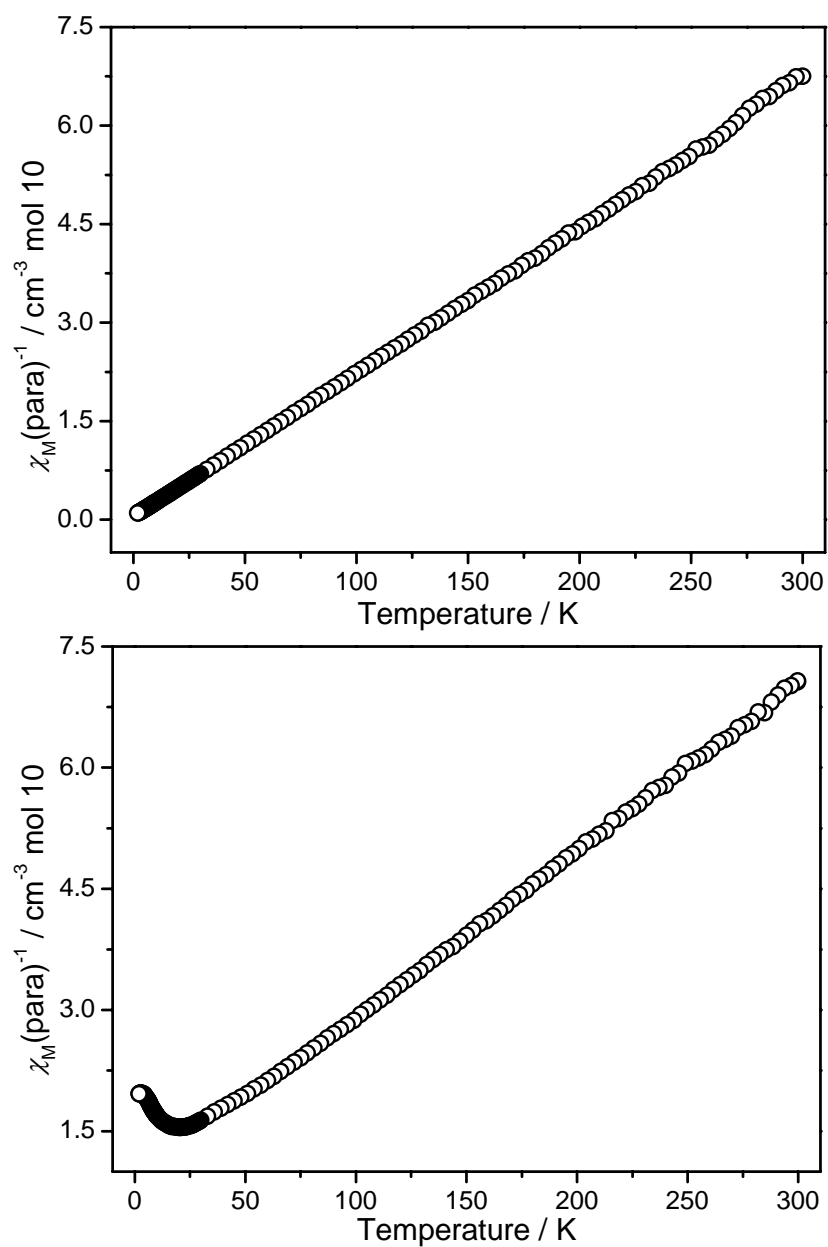


**Figure S8.** Reciprocal paramagnetic susceptibility as function of temperature at  $H = 0.1$  T  
[Mn(NCSe)<sub>2</sub>(pyz)<sub>2</sub>]<sub>n</sub> (**1**; top) and [Mn(NCSe)<sub>2</sub>(pyz)]<sub>n</sub> (**2**; bottom).

## Further experimental details

**Rietveld Refinement.** The Rietveld refinement was performed using *Fullprof2k* with the *Winplotr* software package.<sup>1</sup> The cell parameters were refined with *WinXPOW* Software package.<sup>2</sup> After the initial refinements of the scale factors, unit cell parameters, and profile parameters, the organic part was refined using soft constraints for the pyrazine and selenocyanato ligands. All atoms were refined isotropically and the H atoms were not considered.

**Single-Crystal Structure Analysis.** The investigation was performed with an imaging plate diffraction system (IPDS-2) with Mo-K $\alpha$ -radiation from STOE & CIE. The structure solution was done with direct methods using SHELXS-97<sup>3</sup> and structure refinements were performed against  $|F|^2$  using SHELXL-97.<sup>3</sup> A numerical absorption correction was applied using X-Red Version 1.31 and X-Shape Version 2.11 of the Program Package X-Area.<sup>4</sup> All non-hydrogen atoms were refined with anisotropic displacement parameters. All hydrogen atoms were positioned with idealized geometry and were refined with fixed isotropic displacement parameters [ $U_{\text{eq}}(\text{H}) = -1.2 \cdot U_{\text{eq}}(\text{C})$ ] using a riding model with  $d_{\text{C-H}} = 0.93 \text{ \AA}$ .

**X-ray Powder Diffraction (XRPD).** XRPD experiments were performed using a Stoe Transmission Powder Diffraction System (STADI P) with Cu-K $\alpha$ -radiation ( $\lambda = 154.0598 \text{ pm}$ ) that is equipped with a linear position-sensitive detector (Delta 2 Theta = 6.5-7° simultaneous; scan range overall = 2-130°) from STOE & CIE.

**Differential Thermal Analysis, Thermogravimetry, and Mass Spectroscopy (DTA-TG-MS).** The DTA-TG measurements were performed in a nitrogen atmosphere (purity: 5.0) in

Al<sub>2</sub>O<sub>3</sub> crucibles using a STA-409CD instrument from Netzsch. The DTA-TG-MS measurements were performed with the same instrument, which is connected to a quadrupole mass spectrometer from Balzers via Skimmer coupling from Netzsch. The MS measurements were performed in analogue and trend scan mode in Al<sub>2</sub>O<sub>3</sub> crucibles in a dynamic nitrogen atmosphere (purity: 5.0) using heating rates of 4 °C/min. All measurements were performed with a flow rate of 75 mL/min. The instrument was calibrated using standard reference materials.

**Elemental Analysis.** CHNS analyses were performed using an EURO EA elemental analyzer, fabricated by EURO VECTOR Instruments and Software.

**Spectroscopy.** Fourier transform IR spectra were recorded on a Genesis series FTIR spectrometer, by ATI Mattson, in KBr pellets.

**Magnetic measurements.** Magnetic measurements were performed using a Physical Property Measuring System (PPMS) from Quantum Design, which is equipped with a 9 T magnet. The data were corrected for core diamagnetism.<sup>5</sup>

## References

1. (a) T. Roisnel and J. Rodriguez-Carvajal, in *Proceedings of the Seventh European Powder Diffraction Conference (EPDIC 7)*, eds. R. Delhez and E. J. Mittenmeijer, 2000, pp. 118;  
(b) J. Rodriguez-Carvajal, *Physica B-Condensed Matter*, 1993, **192**, 55.
2. *WinXPOW, Version 2.23*, STOE & CIE GmbH, Darmstadt, Germany, 2003.
3. G. M. Sheldrick, *Acta Cryst.*, 2008, **A64**, 112.
4. *X-Area, Version 1.44, Program Package for Single Crystal Measurements*, STOE & CIE GmbH, Darmstadt, Germany, 2008.



5. G. A. Bain and J. F. Berry, *J. Chem. Educ.*, 2008, **85**, 532.